Silver, E.A., Kimura, G., and Shipley, T.H. (Eds.)
Proceedings of the Ocean Drilling Program, Scientific Results Volume 170

4. Leg 170: Synthesis of Fluid-Structural Relationships of the Pacific Margin of Costa Rica[1]

Eli A. Silver[2]

ABSTRACT

Postcruise scientific investigations based on the results of Leg 170 have made significant inroads into our understanding of flow systems in the largely nonaccretionary subduction setting of the northern Costa Rica subduction zone. With constraints from heat flow, geochemistry, seismic imaging, and the physical properties and fabrics of core materials, we are gaining an understanding of the paths and mechanisms of flow through the décollement and margin wedge, the underthrust sediments, and the uppermost basement of the lower plate. Significant discoveries include estimates of the depth of origin of décollement fluids, rates of flow through the underthrust sediment and the uppermost oceanic crust, the hydraulic separation of the sediment from the uppermost crust, and constraints on the mechanisms driving flow in the basement. These discoveries have opened new avenues for future research.

INTRODUCTION

A poorly understood ocean underlies the seafloor, trapped in fractures and pore spaces of detrital grains and volcanic structures and bound both loosely and tightly by clay and other hydrous minerals. Movement of this ocean is especially significant in active tectonic environments, and huge volumes of fluid move rapidly through subduction systems. A significant part of postcruise studies from Leg 170 focused on this subsurface fluid flow, including structural fabrics and fluid-flow

[1]Silver, E.A., 2000. Leg 170: synthesis of fluid-structural relationships of the Pacific margin of Costa Rica. *In* Silver, E.A., Kimura, G., and Shipley, T.H. (Eds.), *Proc. ODP, Sci. Results,* 170, 1–11 [Online]. Available from World Wide Web: <http://www-odp.tamu.edu/publications/170_SR/VOLUME/CHAPTERS/SR170_04.PDF>. [Cited YYYY-MM-DD]
[2]Earth Sciences Department, University of California, Santa Cruz CA 95064, USA. **esilver@es.ucsc.edu**

Initial receipt: 17 December 1999
Acceptance: 1 June 2000
Web publication: 29 September 2000
Ms 170SR-006

indicators at the interface of subduction. Shipboard results (Kimura, Silver, Blum, et al., 1997) demonstrated that the Costa Rica margin does not undergo frontal accretion and that the bulk of the small, deformed sedimentary wedge at the toe of the margin was not formed by scraping off the incoming sediment from the Cocos plate. Shipboard results also supported the intense fall in heat flow on the Cocos plate (Langseth and Silver, 1996), with major implications for fluid flow. Here I present a synthesis of postcruise science that focused on the structural, chemical, and physical properties relating to fluids at the subduction front and discuss the implications of these results.

STRUCTURAL SETTING OF THE COSTA RICA SUBDUCTION ZONE

The Pacific margin of Costa Rica, offshore of the Nicoya peninsula (Fig. F1), is bathymetrically smooth. The margin's surface is covered by a sedimentary apron (Fig. F2) that varies in thickness from 0.5 to >2 km (Shipley et al., 1992). The apron overlies a deformed prism, composed of relatively high velocity material (Christeson et al., 1999; Ye et al., 1996). Both the prism and the apron are cut by landward-dipping thrust faults in the middle and lower slope region (Fig. F2), which are termed out-of-sequence thrusts (Shipley et al., 1992). Researchers on *Alvin* dives on this margin observed that active fluid venting occurs where these thrusts cut through to the surface (McAdoo et al., 1996; McIntosh and Silver, 1996). The lowermost 5 km of the margin is a deformed sedimentary wedge, also with landward-dipping thrusts. At Ocean Drilling Program drilling Sites 1040 and 1043, we documented that the material composing the wedge is not derived predominantly from the incoming sediment on the Cocos plate. Rather, it is more consistent with material recovered at Site 1041 that penetrated most of the sedimentary apron about 8 km upslope from Site 1040 (Kimura, Silver, Blum, et al., 1997). Postcruise studies by Valentine et al. (1997) have shown that the wedge material is very low in ^{10}Be, indicating a relatively old age for the deformed wedge.

The age-depth curves from reference Sites 1039 and 1040, 1.6 km upslope from the toe, show the same distribution, with zero age sediments directly underlying the décollement. Careful examination of resistivity and gamma ray logs from logging while drilling (LWD) shows that, wiggle for wiggle, all of the material at Site 1039 is present (somewhat compressed) at Site 1043, 0.5 km upslope from the toe, with the exception of the uppermost 9 m of sediment (Saito, 1997). Even this amount cannot be considered as scraped off, because Site 1039 has 5 m of terrigenous turbidites capping the section. A 3.5-kHz seismic line between the two sites shows that these sediments are removed from the trench axis at the toe, likely due to current scour (Kimura, Silver, Blum, et al., 1997). Moritz et al. (in press) applied the method of a genetically trained neural network to the comparison of LWD data at Sites 1039 and 1043. Excluding the top 5 m of turbidites at Site 1039, as discussed above, they found that no sediment was missing between the reference site and the underthrust sediments at Site 1043.

One hole was drilled through the apron into the prism material at Site 1042 (Fig. F1). At this site we recovered at least 60 m of prism material beneath the apron. Microfossils recovered from the prism showed several age inversions, indicating the presence of several thrust sheets,

F1. Location of seismic data and drill sites off northern Costa Rica, p. 10.

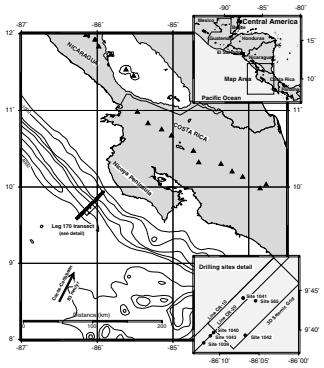

F2. Depth-converted seismic section CR-20, p. 11.

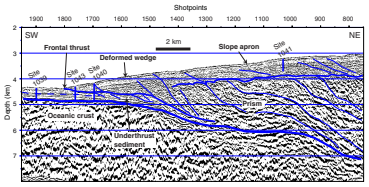

with rock ages ranging from early to late Miocene age. These thrust sheets contained calcarenitic breccias and fragments of mafic rocks and chert (Kimura, Silver, Blum et al., 1997), indicating a provenance different from that of the incoming Cocos plate stratigraphy. These rocks are consistent with exposures onshore, with some derivation from the Nicoya complex and related rocks. In addition, measurements of seismic velocities within these breccias gave values of 4 km/s (Kimura, Silver, Blum, et al., 1997), consistent with the results of wide-angle refraction studies (Christeson et al., 1999). The drilling results are also consistent with the seismic reflection data, showing a significant amount of thrusting in the prism beneath the lower slope and especially a concentration of faulting at the intersection of the prism and the deformed sedimentary wedge (Fig. F2) (see also McIntosh and Sen, 2000).

When we combine the drilling results with the seismic reflection and refraction data, a view emerges of the prism material as follows. The upper slope part of the prism has a high seismic velocity, with no discernible change between the slope region and the onshore area underlain by the Nicoya complex. Thus the upper part of the prism very likely comprises Nicoya complex rocks. Deformation in the upper slope region is by normal faulting (McIntosh et al., 1993), whereas the middle and lower slope regions are characterized by thrust faulting. Seismic velocities decrease downslope, implying that the thrust faults either break up the prism and diminish elastic properties through fracture and alteration or that lower velocity sedimentary material is interthrust with the higher velocity rocks. In the event of the latter alternative, the low-velocity material could consist of sediment that was either deposited originally on the slope apron or underplated beneath the prism, then thrust into it. In addition, the nature of the prism material may change downslope, with more of a detrital (breccia) component deposited seaward of the Nicoya igneous rocks. It is likely that a combination of the above mechanisms acts to vary the measured seismic velocities.

The underthrust Cocos plate stratigraphy plays a significant role in the evolution of the margin. Although offscraping does not come into play at the toe of the slope, McIntosh and Sen (2000) have discovered evidence (also reported by Shipley et al., 1992) for some underplating at depth in the seismic records. One example is subtly illustrated in Figure F2, just to the right of the arrow pointing to "underthrust sediment." Here a mass of material several hundred meters thick and about 1 km wide appears to be underplated beneath the deformed wedge. The underthrust sediment, especially the upper hemipelagic layer, is significantly reduced in thickness from that in the trench because of the load of the deformed wedge and the fact that the uppermost high-porosity strata are all underthrust beneath the toe (Kimura, Silver, Blum, et al., 1997). McIntosh and Sen (2000) have carefully mapped the variation in thickness of the hemipelagic layer with depth beneath the wedge on depth-migrated seismic sections. They find significant thickening of this layer several kilometers landward of the trench axis, an observation explicable by internal deformation of the underthrust hemipelagic sediment. Strongly supporting this observation is the finding during Leg 170 that steeply dipping strata were measured in the underthust hemipelagic layer at both Sites 1040 and 1043 (Kimura, Silver, Blum, et al., 1997). The zone of anomalously steep dips includes the entire hemipelagic section at Site 1040 and the upper part of the section at Site 1043. There is some indication of landward dips cutting the strata in the underthrust section in Figure F2.

PERMEABILITY STRUCTURE OF LEG 170 CORES

Studies of the variation in permeability with deformation have been carried out by Saffer et al. (2000) and Bolton et al. (**Chap. 3,** this volume), the latter using significant structural input from Vannucchi and Tobin (2000). Vannucchi and Tobin (2000) documented deformation patterns in the deformed sediment wedge, the décollement zone, and the underthrust sediment package. Deformation in the deformed wedge occurs through the development of kink bands and shear bands, with both bedding-parallel and bedding-oblique bands cutting across each other. The kink and shear bands illustrate deformation associated with loss of porosity. The alternation of bedding-parallel and bedding-oblique structures implies the possibility of more than one separate deformation mechanism; overburden pressure, gravity sliding, and tectonic stress may all have been factors. A finding of a major shear zone at Site 1040 and a regular progression of strain indicating a continuum from vertical to horizontal maximum principal stress suggest the presence of active tectonic compression (Vannucchi and Tobin, 2000).

Deformation and dewatering in the décollement zone appear less systematic than in the wedge, with the presence of alternating low- and high-porosity zones. Silty high-porosity zones alternate with silt and clay low-porosity regions, with smectite alteration of earlier flow channels. These channels suffered porosity collapse and mineral alteration, with the presence of both flattening and shearing structures. The strain and fluid flow regime was episodic, with periodic buildup of overpressures and structural collapse. Deformation bands in the décollement produced hydraulic brecciation. Both a brittle and ductile regime exists in the décollement zone, and the boundary between them has high potential to transmit fluid (Vannucchi and Tobin, 2000).

Faults are present in the underthrust section as well, but these are narrow, discrete features or braided arrays, with no ductile structures. Most faults show reverse movement. Fault density decreases toward the base of the underthrust section. Deformation bands focused in the upper part of the underthrust section may be dewatering pathways, explaining the mechanism for the much higher porosity loss in the upper hemipelagic layer. Incipient stylolite development and recrystallization, which indicate pressure solutions, characterize the pelagic limestone layer. The basal sediments have a very different structure, with normal faulting dominating, probably a result of spreading ridge processes. At Site 1039, both quartz and calcite precipitate as close as 20 m from the base of the sediments but do not precipitate nearer to the gabbros, suggesting a separate fluid circulation system associated with the gabbros (Vannucchi and Tobin, 2000).

Bolton et al. (**Chap. 3,** this volume) and Saffer et al. (2000) have each shown a linear relationship between permeability and porosity. Bolton et al. demonstrated this for the deformed wedge and Saffer et al. for the underthrust sediment. Paths of permeability vs. effective stress were quite different for the different structural regimes (Bolton et al., **Chap. 3,** this volume). In the deformed wedge, increasing effective stress led to decreased permeability until fracture occurred. Release of effective stress resulted in a permeability drop nearly 5 orders of magnitude. For hard chalk in the underthrust section, very little difference was noted during the stress cycle. For underthrust diatomite and soft clay near the wedge surface, increasing effective stress by 1 MPa led to a decrease in

permeability of roughly a factor of 3–5, recovering with stress release (Bolton et al., **Chap. 3,** this volume).

Saffer et al. (2000) found that the in situ excess pore fluid pressures in the underthrust sediment increased from 1.3 MPa at the top to 3.1 MPa near the base of the section. They inferred from this increase that the uppermost sediments drain most easily, whereas the lower sediments remain undrained. The latter implies that the sedimentary system is uncoupled from the underlying hydrologic system in the upper oceanic basement. Saffer et al. further discovered that the measured permeabilities are a factor of about 100 too low to explain the dewatering rates implied by the rate of change of thickness of the underthrust hemipelagic layer. Barring experimental error, they suggest that a combination of narrow, high-permeability horizons within the hemipelagic (probably ash) layers and local vertical dewatering conduits can explain the measurement vs. modeling discrepancy.

IMPLICATIONS OF HEAT FLOW AND GEOCHEMISTRY FOR FLUID FLOW

Geochemical analyses of pore fluids in the décollement and overlying deformed sedimentary wedge indicate fluid origins from deep within the subduction system. Potassium and lithium concentrations and polymerized hydrocarbons indicate formation temperatures of between 100° and 150°C (Kimura, Silver, Blum et al., 1997; Chan and Kastner, 1998). Using the measured heat flow at Site 1041 and a conservative value for deep crustal thermal conductivity, Silver et al. (2000) suggest maximum depths of origin of 10–15 km, or locations along the décollement 40–60 km from the trench. Profiles of chlorinity and salinity through the deformed wedge at Site 1040 and the slope apron at Site 1041 both show significantly lower values than that of seawater, indicating freshening by several sources. One source is flow from listric thrust faults that root in the décollement. Significant local excursions of freshening are seen in such conduits. Another source of local freshening is gas hydrates (Kimura, Silver, Blum, et al., 1997; Kopf et al., 2000), which are abundant at both sites. A third alternative that was not evaluated is influx of meteoric water through the apron from land sources.

From surface heat flow measurements, Langseth and Silver (1996) documented very low heat flow on the incoming Cocos plate and only slightly increased heat flow over the middle to lower slope region. Their findings were corroborated by downhole temperature measurements during Leg 170, at Sites 1039, 1040, and 1041 (Kimura, Silver, Blum et al., 1997). In fact, heat flow values measured downhole were uniformly lower than those measured at the surface. Ruppel and Kinoshita (2000) carried out a careful analysis of the Leg 170 heat flow data, finding similar results, though values are slightly adjusted from those reported by Kimura, Silver, Blum, et al. (1997). They explained the difference between surface and borehole heat flow by nonlinear perturbation of the thermal regime by advective flux, which was strongest at Site 1040 and weakest at Site 1041. In the gas hydrate zone, above the décollement zone, Ruppel and Kinoshita (2000) find a vertical advective flux rate of 5–7 mm/yr at Site 1040, less than 1 mm/yr at Site 1041, and 19 mm/yr in the hemipelagic sediments at Site 1039. The high vertical flux rates for Site 1040 may be facilitated by fracture permeability.

Langseth and Silver (1996), following suggestions by Langseth and Herman (1981) and Yamano and Uyeda (1990), proposed that flow of seawater into the uppermost oceanic crust was the most likely explanation for the drastic lowering of heat flow from expected equilibrium values. During Leg 170, geochemical profiles at Site 1039 showed marked changes in gradient for numerous chemical species, including Ca, Mg, Sr, Li (Chan and Kastner, 1998) and other elements, moving rapidly toward seawater values near the base of the sediment pile (Kimura, Silver, Blum, et al., 1997). Using the gradients for Sr and Li concentration and isotope ratio gradients, the formation of the basement water is found to be younger than 15 k.y. (Li) or 20 k.y. (Sr).

To estimate the possible driving mechanism for fluid flow in the crust, Silver et al. (2000) used an analytical thermal model from Fisher and Becker (1999), in which temperature differences between sites of recharge and discharge of fluids are responsible for driving the flow. Unknowns included the permeability and thickness of the zone of crustal flow and the distance between sites of discharge and recharge. By assuming a temperature difference of 52°, permeability ranging between 10^{-9} and 10^{-14} m^2, and pressure differences of 80 to 230 kPa between recharge and discharge sites, they found that specific discharge is in the 1 to 5 m/yr range and ages of basement water are in the 2- to 16-k.y. range, generally consistent with the geochemical model. Lower pressure difference between sites, caused by loss of head during vertical flow or lower temperature differences between recharge and discharge sites, requires the permeabilities to be higher for sustained flow. Alternatively, an additional driving force could be active along with temperature differences, which would allow lower permeabilities (indeed, the permeabilities measured in the sediment section were lower).

One potential source of additional driving force is cyclic seismic flexure and associated crack dilation and contraction, as suggested by Sibson (1994) and Muir-Wood (1994). Crack dilation is expected to be associated with interseismic strain on the trench outer wall, allowing entrance of water into the uppermost crust. During coseismic periods, fluids would be forced to flow, and a component of flow might be along the trench axis (Silver et al., 2000). Whether such a mechanism has any significance remains to be tested through additional drilling and a much more extensive network of heat-flow observations.

SUMMARY

Fluid flow occurs in several different systems in the Costa Rica subduction zone. One is a sediment and upper plate system, which is itself composed of three subunits. The structurally lowest sediment subunit is composed of the underthrust sediments. As they thrust beneath the upper plate, they are rapidly dewatered. Flow occurs several orders of magnitude more rapidly than is expected from measured permeabilities in cores, suggesting that flow is localized along narrow, high-permeability channels and probably exits to the décollement or the seafloor through spaced, vertical conduits. Overpressures that increase with depth in the underthrust section imply little or no communication with the deeper system, discussed below.

The next regime of flow is the décollement. Structurally, this zone is marked by closely spaced shear bands, some filled with secondary smectite, which indicate collapsed former flow paths. The décollement appears structurally to develop by episodic flow and collapse, decreasing

porosity, and increasing shear fabrics. Geochemically, the décollement shows a significant decrease in chlorinity, likely due to clay mineral dehydration with depth. The concentrations of K and Li suggest temperatures of 100°–150°C, equivalent to depths of 10–15 km, or distances of 40–60 km landward of the trench. Flow also occurs from the décollement to the deformed sedimentary wedge, where local fractures show very low chlorinity. In general, both the deformed sedimentary wedge and the slope apron show overall lower salinity and chlorinity than seawater values because of a combination of local formation and melting of gas hydrates and fluid influx from the décollement.

The second major flow system occurs in the upper part of the oceanic basement, inferred because of the extreme decrease in heat flow over that expected for conduction and the discovery that chemical species such as Ca, Mg, Li, Sr, K, and others show a rapid change in gradient near the basement interface, moving close to seawater values. Geochemical modeling indicates basement fluid ages of 15 to 20 k.y., and thermal models predict specific discharge rates in the range 1 to 5 m/yr. Such discrepancies represent the range of uncertainty due to lack of specific knowledge of permeabilities, layer thicknesses, driving forces, and recharge-discharge distances. Driving forces probably include temperature differences between the recharge and discharge zones, and in this location may include the addition of cyclic seismic flexure opening and closing flow pathways through a seismic cycle.

ACKNOWLEDGMENTS

I am grateful for the effort and support of the scientific party, technical staff and crew of Ocean Drilling Program Leg 170. It has been a great privilege to carry out postcruise science with my close coworkers, including Miriam Kastner, Kirk McIntosh, Andy Fisher, Demian Saffer, and Julie Morris. I am especially grateful to have had the opportunity to work with Mark Langseth prior to Leg 170. His foresight has played a key role in our work. I thank Joris Gieskes and Gail Christeson for helpful reviews. This work was supported by the generosity of the JOI/US Science Support Program, through co-chief scientist support and grant 170-F000511.

REFERENCES

Chan, L.-H., and Kastner, M., 1998. Lithium isotopic composition of fluids and sediments at the Costa Rica subduction zone: results from ODP Sites 1039 and 1040. *Eos,* 79:395.

Christeson, G.L., McIntosh, K.D., Shipley, T.H., Flueh, E., and Goedde, H., 1999. Structure of the Costa Rica convergent margin, offshore Nicoya peninsula. *J. Geophys. Res.,* 104:25443–25468.

DeMets, C., Gordon, R.G., Argus, D.F., and Stein, S., 1994. Effect of recent revisions to the geomagnetic reversal time scale or estimates of current plate motions. *Geophys. Res. Lett.,* 21:2192–2194

Fisher, A.T., and Becker, K., 2000. Reconciling heat flow and permeability data with a model of channelized flow in oceanic crust. *Nature,* 403:71–74.

Kimura, G., Silver, E.A., Blum, P., et al., 1997. *Proc. ODP, Init. Repts.,* 170: College Station, TX (Ocean Drilling Program).

Kopf, A., Deyhle, A., and Zuleger, E., 2000. Evidence for deep fluid circulation and gas hydrate dissociation using boron and boron isotopes in forearc sediments from Costa Rica (ODP Leg 170). *Marine Geology,* 167: 1–28.

Langseth, M.G., and Herman, B.J., 1981. Heat transfer in the oceanic crust of the Brazil basin. *J. Geophys. Res.,* 86:10805–10819.

Langseth, M.G., and Silver, E.A., 1996. The Nicoya convergent margin: a region of exceptionally low heat flow. *Geophys. Res. Lett.,* 23:891–894.

McAdoo, B.G., Orange, D.L., Silver, E.A., McIntosh, D., Abbott, L., Galewsky, J., Kahn, L., and Protti, M., 1996. Seafloor structural observations, Costa Rica accretionary prism. *Geophys. Res. Lett.,* 23:883–886.

McIntosh, K.D., and Sen, M.K., 2000. Geophysical evidence for dewatering and deformation processes in the Ocean Drilling Program Leg 170 area offshore Costa Rica. *Earth Planet. Sci. Lett.,* 178:125–138.

McIntosh, K.D., and Silver, E.A., 1996. Using 3D seismic reflection data to find fluid seeps from the Costa Rica accretionary prism. *Geophys. Res. Lett.,* 23:895–898.

McIntosh, K.D., Silver, E.A., and Shipley, T., 1993. Evidence and mechanisms for forearc extension at the accretionary Costa Rica convergent margin. *Tectonics,* 12:1380–1392.

Moritz, E., Bornholdt, S., Westphal, H., and Meschede, M., in press. Sediment subduction lacking accretion at the Costa Rica convergent margin (Ocean Drilling Program Leg 170). *Earth Planet. Sci. Lett.*

Muir Wood, R., 1994. Earthquakes, strain-cycling and the mobilization of fluids. *In* Parnell, J. (Ed.), *Geofluids: Origin, Migration and Evolution of Fluids in Sedimentary Basins*. Geol. Soc. Spec. Publ. London, 78:85–98.

Ruppel, C., and Kinoshita, M., 2000. Heat, fluid, and methane flux on the Costa Rican active margin off the Nicoya peninsula. *Earth Planet. Sci. Lett.,* 179:153–165.

Saffer, D.M., Silver, E.A., Fisher, A.T., Tobin, H., and Moran, K., 2000. Inferred pore pressures at the Costa Rica subduction zone: implications for dewatering processes. *Earth Planet. Sci. Lett.,* 177:193–207.

Saito, S., 1997. In-situ physical properties of the Costa Rica and Barbados subduction systems. *Eos,* 78:F686.

Shipley, T.H., McIntosh, K.D., Silver, E.A., and Stoffa, P.L., 1992. Three- dimensional seismic imaging of the Costa Rica accretionary prism: structural diversity in a small volume of the lower slope. *J. Geophys. Res.,* 97:4439–4459.

Sibson, R., 1994. Crustal stress, faulting and fluid flow. *In* Parnell, J. (Ed.), *Geofluids: Origin, Migration and Evolution of Fluids in Sedimentary Basins*. Geol. Soc. Spec. Publ. London, 78:69–84.

Silver, E.A., Kastner, M., Fisher, A.T., McIntosh, K.D., and Saffer, D.M., 2000. Fluid flow paths in the Middle America Trench and Costa Rica margin. *Geology,* 28:679–682.

Valentine, R., Morris, J.D., and Duncan, D., 1997. Sediment subduction, accretion, underplating and arc volcanism along the margin of Costa Rica: constraints from Ba, Zn, Ni, and ^{10}Be concentrations. *Eos,* 78:F673.

Vannucchi, P., and Tobin, H., 2000. Deformation structures and implications for fluid flow at the Costa Rica convergent margin, Ocean Drilling Program Sites 1040 and 1043, Leg 170. *J. Struct. Geol.,* 22:1087–1103.

Yamano, M., and Uyeda, S., 1990. Heat-flow studies in the Peru Trench subduction zone. *In* Suess, E., von Huene, R., et al., *Proc. ODP, Sci. Results,* 112: College Station, TX (Ocean Drilling Program), 653–661.

Ye, S., Bialas, J., Flueh, E.R., Stavenhagen, A., von Huene, R., Leandro, G., and Hinz, K., 1996. Crustal structure of the Middle America Trench off Costa Rica from wide-angle seismic data. *Tectonics,* 15:1006–1021.

Figure F1. Locations of seismic data and drill sites off northern Costa Rica. The inset on the lower right shows detail of the drill sites. The arrow shows the direction and rate of relative plate motion (DeMets et al., 1994). Triangles onshore = volcanoes. Contour interval offshore = 1000 m.

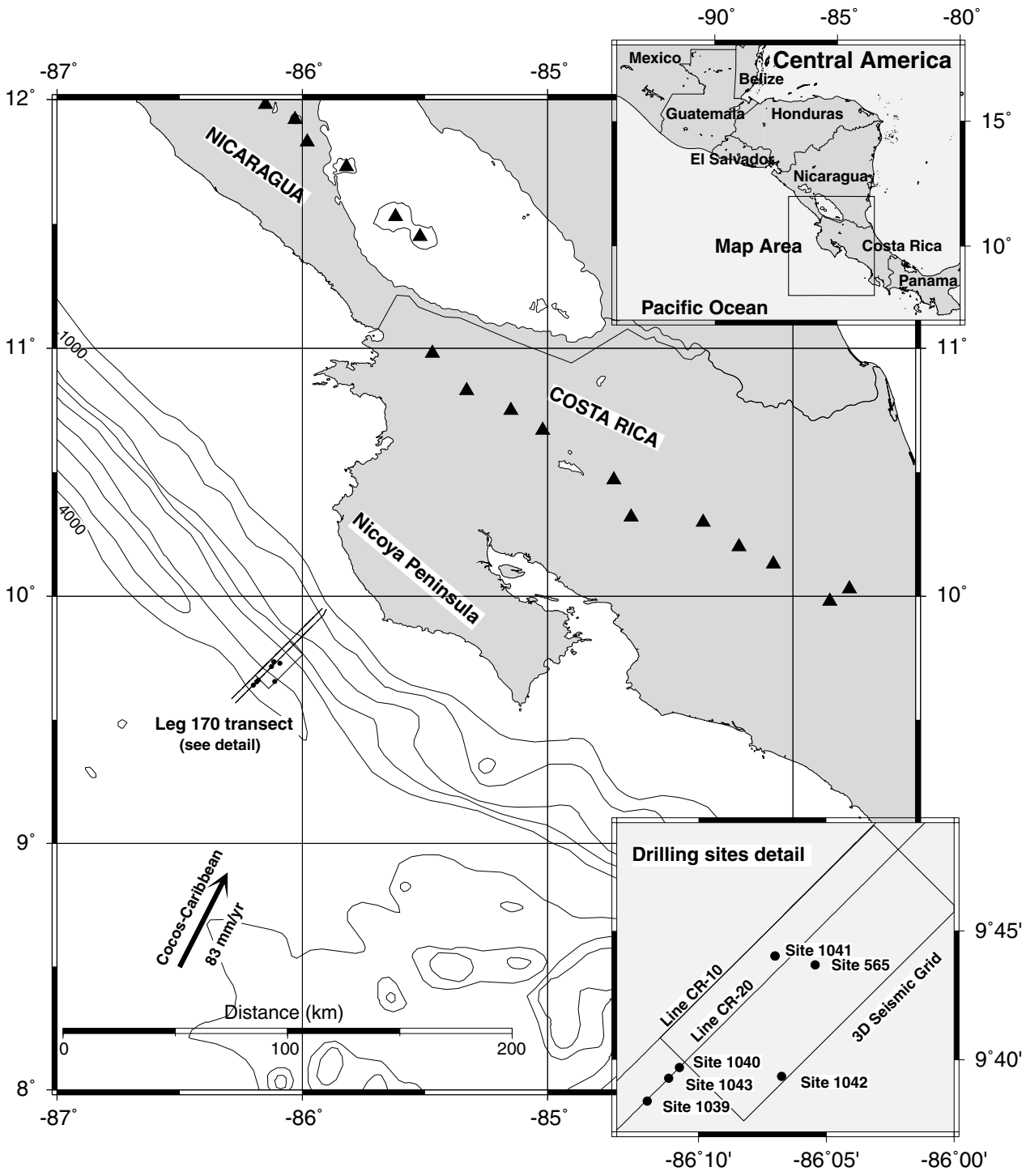

Figure F2. Depth-converted seismic section CR-20, crossing Sites 1039, 1040, 1041, and 1043. Processing and depth conversion are by K.D. McIntosh, based on seismic velocities from Christeson et al. (1999). Heavy lines are interpreted unit boundaries or faults. Most faults upslope from the frontal thrust outcrop are out-of-sequence thrusts. These later faults cut the prism, the slope apron, the deformed wedge, and even the underthrust sediments.